Bulg. J. Phys. **44** (2017) 509–519

Combined Quantum Kinetic and Rate Equations Modeling of the Non-Equilibrium Carrier Dynamics of Matter Exposed to X-Ray Laser Pulses

T. Apostolova[1,2], **E. Oliva**[3]
[1]Institute of Nuclear Research and Nuclear Energy, Bulgaria
[2]Institute for Advanced Physical Studies, New Bulgarian University, 1618 Sofia, Bulgaria
[3]Instituto de Fusion Nuclear, Universidad Politecnica de Madrid, Spain

Received *6 November 2017*

Abstract. Nanoplasma generation in neon clusters irradiated by intense X-ray femtosecond laser pulse is described using a generalized Maxwell Boltzmann Bloch quantum-kinetic formalism coupled self-consistently with rate equations which describe the creation of unoccupied atomic core levels. The generation of dense hot plasma environment lasting longer than the driving laser pulse together with the simultaneous creation of unoccupied core levels is studied as an initial step to explore the process of nuclear excitation by electron capture. The results describing the microscopic laser-induced carrier dynamics and the secondary interaction of the emitted soft X-rays with the perturbed clusters might provide essential insights on the triggering conditions of this exotic nuclear excitation mechanism.

1 Introduction

Irradiation of matter in gaseous and solid phase with intense femtosecond-pulsed X-ray lasers leads to high electron excitation and high non-equilibrium carrier dynamics. As a result, spatially confined dense electron-hole plasma is created which relaxes on a femtosecond to picosecond time scale together with the production of atomic charged states [1].

Transferring energy from plasma electrons to atomic nuclei [2, 3] proves to be an efficient nuclear excitation mechanism [4] in which a nucleus is excited by a virtual photon emitted when an electron is captured from the continuum to a vacant atomic level of the formed ions. The present work provides initial results for plasma generation from deeply bound electrons and the subsequent plasma evolution, based on a self-consistent approach which treats these processes and the atomic level occupancies on the same footing.

Intense short laser pulses-cluster interaction creates small-scale plasmas (nanoplasmas) [5]. These nanoplasmas are transient, but they allow the investigation of fundamental laser-matter interaction processes such as ionization and laser energy absorption mechanisms. As conglomerations of condensed matter, with sizes ranging from 10^2 to 10^6 atoms, clusters are intermediate to macroscopic condensed matter and microscopic systems, such as atoms and molecules, thus allowing these processes to be investigated as a function of system size.

The unique properties of XFEL such as high photon flux and high intensity enable the multiple photoionization of all atoms in the focal spot of the beam simultaneously, followed by multiple secondary excitation and relaxation. Tunable wavelengths of XFELs are also of great importance for the purpose of creating vacant charged states. The time scales of typical free electron laser radiation are of the order of some 10 fs and those of hollow ion transitions scale down to 1 fs.

Since the energy deposition occurs on the time scale of the duration of the XFEL pulse and is much faster than any hydrodynamic motion, the microscopic description of the non-equilibrium dynamics of the system is of great importance and is provided by our approach. The problem which we are solving consists of describing the transient bound electron occupancies along with the evolution of the continuum plasma electrons. The dynamics of each subsystem is governed by processes affecting the electrons within both subsystems as well as by processes which transfer electrons from one subsystem to the other one. The evolution of the bound state electrons is determined by the time-dependent rate equations. Because of the intense free-bound and bound-free electron transitions these equations should be solved simultaneously with generalized Maxwell Boltzmann Bloch kinetic approach instead of Boltzmann equation used previously [6]. The exchange of electrons starts from the highly nonequilibrium state when the laser energy is deposited on a femtosecond time scale into the electron system, until a few tens of picoseconds later when the highly excited electrons relax and thermalize. In our initial calculations the coefficients of the rate equations corresponding to a time varying electron energy distribution function are determined self-consistently by the solution to the Boltzmann equation [7, 8]. The formalism of Maxwell Boltzmann Bloch kinetic equation used to describe the plasma, includes the initial inner shell photo-ionization processes, radiative recombination, additional collisional ionization and three body recombination. The electron energy distribution function (EEDF) of the excited electrons emerging from the interplay of these processes is a solution of this equation. This approach is applicable to plasmas in conventional materials as well as to nanoplasmas.

2 Theoretical Model

The methodology described in this section is intended to model the interaction of intense X-ray pulses with noble gas clusters and atoms, the subsequent evolution

of the generated nanoplasma, the propagation of the soft X-rays emitted by the perturbed atoms and clusters and their secondary interaction with the perturbed clusters. In order to fully describe this complex scenario we need rate equations to study the photoionization and subsequent relaxation of clusters leading to the generation of the nanoplasma;Boltzmann equation for the temporal dynamics of unbound electrons that compose the nanoplasma; Maxwell-Bloch equations to study the radiative relaxation of the created ions and the propagation of the emitted soft X-rays; Boltzmann-Bloch equations for electrons and holes in clusters to study the interaction of the emitted soft X-rays with unrelaxed clusters. This approach will be described in full in the following subsections. Ceratin approximations and simplifications will be used to obtain initial results illustrating how the model works.

2.1 Generalized Maxwell Boltzmann Bloch equations-electrons in the continuum

The complete set of equations describing the dynamics of interband coherence and populations of electrons and holes as in a two-band model for materials with a valence and conduction bands are the Maxwell-Boltzmann-Bloch equations [9–11]

$$\frac{\partial}{\partial t}f^{\alpha}(\vec{k},\vec{r},t)+\frac{1}{\hbar}\frac{\partial\varepsilon^{\alpha}(\vec{k},\vec{r})}{\partial k}\frac{\partial f^{\alpha}(\vec{k},\vec{r},t)}{\partial r}-\frac{1}{\hbar}\frac{\partial}{\partial r}[\delta\varepsilon^{\alpha}(\vec{k},\vec{r})+q\Phi(r)] \times\frac{\partial f^{\alpha}(\vec{k},\vec{r},t)}{\partial k}=\Gamma^{\alpha}(\vec{k},\vec{r},t)+\frac{\partial}{\partial t}f^{\alpha}(\vec{k},\vec{r})_{\text{col}} \quad (1)$$

$$\frac{\partial}{\partial t}p(\vec{k},\vec{r},t)=-\frac{i}{\hbar}[\varepsilon^{e}(\vec{k},\vec{r},t)+\varepsilon^{h}(-\vec{k},\vec{r},t)]p(\vec{k},\vec{r},t)- - i\Omega(\vec{k},\vec{r})[f^{e}(\vec{k},\vec{r},t)+f^{h}(-\vec{k},\vec{r},t)-1]+\frac{\partial}{\partial t}p(\vec{k},\vec{r})_{\text{col}} \quad (2)$$

with generation rate induced by the laser electric field $\Gamma^{\alpha}_{ef} = i\left[\Omega(\vec{k},\vec{r})p^{*}(\vec{k},\vec{r})-\Omega^{*}(\vec{k},\vec{r})p(\vec{k},\vec{r})\right]$, where $\Omega(\vec{k},\vec{r})$ is the renormalized Rabi frequency defined by $\hbar\Omega(\vec{k},\vec{r})=\mu(\vec{k})E(\vec{k},\vec{r}))+\sum_{\vec{k}'}p(\vec{k}',\vec{r})V^{s}_{\vec{k}'-\vec{k}}$. The first term is the product of the dipole moment and electric field while the second is the internal field responsible of Coulomb enhancement. $\Gamma^{\alpha}=\sum\Gamma^{\alpha}_{i}$ includes all processes taken into account in our calculation such as coherent interaction with electric field, photoionization, radiative recombination, impact ionization and three body recombination. Collisional contributions $\frac{\partial}{\partial t}f^{\alpha}\left(\vec{k},\vec{r}\right)_{\text{col}}$ lead to relaxation in the carrier distributions and decay in the interband polarization.

The electric field $\vec{E}(\vec{r},t)$ follows Maxwell's wave equation. When applying both paraxial and slowly varying envelope approximation, the resulting equation is as

follows:

$$\frac{\partial E}{\partial z} + \frac{n}{c}\frac{\partial E}{\partial t} = \frac{i}{2k_z}\nabla_\perp^2 E + \frac{i\omega_L}{2\epsilon_0 c}P\,. \tag{3}$$

In the equations above P is the macroscopic polarization, computed from the microscopic as $P = \mu\sum_k p(k)$, $f^{\alpha=e,h}$ are the distribution functions for electrons and holes, $\vec{k}$ and $\vec{r}$ are the three-dimensional vectors in momentum space and real space, Φ is the electrostatic potential, ε^α are the renormalized energies, n is the refractive index of the medium and k_z and ω_L are respectively the wavenumber and frequency of the laser electric field.

Keeping the zeroth-order spatial derivatives of the distribution functions, and eliminating the polarization by solving Eq.(2) where the collisional terms have been neglected within the adiabatic and Markov approximations [10], the equations of motion for electron and hole distribution functions are given by the generalized Boltzmann equations with semiclassical generation rates. [11]. Based on these approximations the dynamics of the unbound electrons is investigated using the generalized Boltzmann equation [7, 8, 12].

2.2 Rates

Below we describe the rates used in the equations for bound states and the ones used into the equation for the continuum.

2.2.1 Photoionization

From reference [13] the rate of photoionization for level i is

$$\Gamma_{PI,i}(t) = \sigma_i^{PI}(\hbar\omega_X)J_X(t) \tag{4}$$

with

$$J_X(t) = \frac{I(t)}{\hbar\omega_X}\,, \tag{5}$$

where $\hbar\omega_X$ is the photon energy, $\sigma_i^{PI}(\hbar\omega_X)$ is the photoionization cross section of the level calculated from atomic code [14]. The driving laser field strength is given in terms of intensity $I(t)$ of the X ray by

$$\mathcal{E}(t) = \sqrt{\frac{2I(t)}{c\varepsilon_0}}\,. \tag{6}$$

For Gaussian pulse

$$I_t\,(t) = I_0 \exp\left[-t^2/\tau_L^2\right],$$

where τ_L is the pulse duration.

2.2.2 Radiative recombination

The spontaneous emission term for level i is given by the expression [15]

$$\Gamma_{RR,i}(t) = \frac{\omega_t^3 p^2}{3c^3\epsilon_0\pi\hbar}\,, \tag{7}$$

where ω_t is the transition frequency between two levels with the transition energy given by $E_t = \hbar\omega_t$ and p is the dipole moment also calculated from atomic code [14].

2.2.3 Auger process, impact ionization and three body recombination

For the time-independent Auger process rate we use the expression derived for the atomic case [16].

The collision integral corresponding to electron impact ionization rate can be calculated as [17]

$$\Gamma_{CI,i} = \frac{N}{\Delta E} f_i \int_{E_i-1/2\Delta E}^{E_i+1/2\Delta E} \int_{E_j-1/2\Delta E}^{E_j+1/2\Delta E} E^{1/2}\sigma^{CI} dE dE_1\,, \tag{8}$$

where σ^{CI} is the impact ionization cross section.

In the non-equilibrium case the principle of detailed balance cannot be applied. The three body recombination rate is

$$\Gamma_{TBR,i} = \frac{N}{\Delta E} f_i f_j \int_{E_i-1/2\Delta E}^{E_i+1/2\Delta E} \int_{E_j-1/2\Delta E}^{E_j+1/2\Delta E} E^{1/2} E_1^{1/2}\sigma^{TBR} dE dE_1\,, \tag{9}$$

where σ^{TBR} is the three body recombination cross section, f_i is the function $f(E,t)$ evaluated at some electron energy $E := E_i$ and $f(E,t) = f(E_i,t)$ on the interval $[E_i - \frac{1}{2}\Delta E, E_i + \frac{1}{2}\Delta E]$ and N is the ion number.

2.3 Electrons in bound states

The set of bound electrons at a given time represents an atomic configuration and the dynamics of bound electrons is obtained by following the time-dependence of any electron configuration of the atom. The time-dependent changes between different possible configurations is given by time-dependent rate equation (TDRE). The evolution of configurations may start from the neutral atom and may finish with a fully ionized atom.

When the energy levels that appear in the medium can be considered as atomic levels, the equation for the polarization can be written as

$$\frac{\partial P}{\partial t} = \Gamma - \gamma P - \frac{i\mu}{\hbar} E\left(N_u - N_l\right),$$

where Γ is a stochastic source term with vanishing correlation time that models the spontaneous emission, γ is the depolarization rate and N_u, N_l are respectively the populations of the upper and lower level of the transition. These populations are computed by solving the corresponding rate equations for each level N_i

$$\frac{\partial N_i}{\partial t} = \sum_k C_{ki} N_k \pm \Im\left(E^* P\right) \frac{1}{2\hbar} ,$$

where the summation is extended to all levels taken into account; $i = u, l$ and C_{ki} are the excitation and deexcitation rates. Photoionization, radiative recombination, Auger recombination, impact ionization and three body recombination rates have already been described in the previous section. Collisional excitation and deexcitation rates are computed using the nanoplasma electron distribution function and the cross section σ_{ij}^{ce}

$$C_{ij} = n_e \langle \sigma_{ij}^{ce} v \rangle = n_e \int_{\Delta E}^{\infty} \sqrt{\frac{2E}{m_e}} \sigma_{ij}^{ce}(\epsilon) \, , f^e(\epsilon) d\epsilon \, .$$

When the electron distribution function can be assumed as a Maxwellian, collisional rates can be computed by using Van Regemorter's rates [21]

$$C_{ij} = 1.6 \times 10^{-5} \frac{f_{ij} \langle g \rangle}{\Delta E_{ij} \sqrt{k T_e}} e^{-\frac{\Delta E_{ij}}{k T_e}} ,$$
$$C_{ji} = \frac{\gamma_i}{\gamma_j} C_{ij} e^{\frac{\Delta E_{ij}}{k T_e}} ,$$

where f_{ij} is the oscillator strength, $\langle g \rangle$ the Gaunt factor, ΔE_{ij} the difference of energy between levels i and j, k Boltzmann's constant, T_e the electron temperature and γ_i and γ_j the degeneracies of each level.

3 Results

In this section show some preliminary results obtained with a simplified version of the model aforementioned. We have studied the interaction of a short (200 fs), intense ($I = 10^{18}$ W cm^2) X-ray pulse ($\hbar\omega = 2$ keV) with Neon gas ($n_0 = 10^{22}$ cm^{-3}) and Neon clusters [18]. The energy of the photons is high enough to ionize a core $1s^2$ electron (the energy of the photoelectron is 1123 eV), leaving the Ne^{1+} ion in an excited state $1s^1 2s^2 2p^6$ that can decay radiatively to the ground state of Ne^{1+} $1s^2 2s^2 2p^5$ or via an Auger process to the ion Ne^{2+}. The energy of the Auger electron is 810 eV. The ground state of Ne^{1+} can also be photoionized to Ne^{2+}, emitting an electron with an energy of 1094 eV. The cross-sections for the photoionization of Ne atoms and Ne^{1+} ions are $\sigma_{K^2 L^8 K^1 L^8} = 4.06 \cdot 10^{-20}$ cm^{-2} [17]. and $\sigma_{K^2 L^7 K^1 L^7} = 4.05 \cdot 10^{-20}$ cm^{-2} [19] respectively. The Auger rate of the

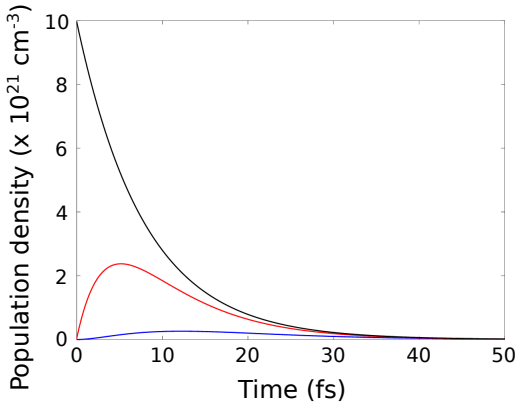

Figure 1. (color online) Population of the ground state of Ne ($1s^2 2s^2 2p^6$, black), the ground state of Ne^{1+} ($1s^2 2s^2 2p^5$, blue) and the excited level of Ne^{1+} ($1s^1 2s^2 2p^6$, red).

excited state of Ne^{1+} is $A_{K^1L^8K^2L^6} = 2.74 \cdot 10^{14}$ s^{-1} while the radiative rate to the fundamental level is $A_{21} = 2,185 \cdot 10^{12}$ s^{-1}. The corresponding non-diagonal matrix element of the dipole is $\mu = 4.9172 \cdot 10^{-31}$ C m.

The fact that X-ray photons are energetic enough to ionize inner core electrons allows us to use the same model to treat photoionization and Auger process in atoms and clusters since the band structure related to the cluster size can be neglected for these electrons.

Figure 1 shows the population of each of the three levels taken into account in our model. The ground state of Ne decays exponentially due to photoionization (black line). A significant number of excited Ne^{1+} ions are produced, as depicted in red. These ions have a short lifetime, decaying to Ne^{2+} via an Auger process. A short number can undergo a radiative transition towards the ground state of Ne^{1+}. However, the low probability of this process compared to the Auger one and the further photoionization of the ground state of Ne^{1+} reduces the population of this level, as shown in blue line. A population inversion between the $1s^1 2s^2 2p^6$ and $1s^2 2s^2 2p^5$ levels of Ne^{1+} has been achieved. It is worth mentioning that the population inversion is not reduced by radiative transitions between the excited level and the ground state of Ne^{1+}. Indeed, Auger processes, being faster than radiative recombination, are responsible of the fast depletion of the excited level, while photoionization continuously depletes the ground state of Ne^{1+}. Thus, the population inversion is never negative; the gas has been *bleached* and no further absorption of the X-ray pulse can take place.

Each photoionization and Auger process ionizes an electron with a characteristic energy at an specific rate, $\Gamma_{PI,i}(t) = \sigma_i^{PI}(\hbar\omega_X) J_X(t)$ and $\Gamma_{\text{auger},i}(t) = A_{\text{auger},i} N_i$. These generation terms are fed to the Boltzmann equation for the un-

dound electrons. Line broadening is taken into account when computing the generation term for Boltzmann equation. The full width at half maximum (FWHM) of a natural broadened line is

$$\text{FWHM}_{\text{natural}} = \hbar\Big(\sum A_{im} + \sum_n A_{jn}\Big),$$

where i, j denote the two levels involved in the transition and A_{im}, A_{jn} denote all the radiative decay channels of each level. For Doppler broadening, the FWHM is given by

$$\text{FWHM}_{\text{doppler}} = \frac{\Delta E_{ij}}{\hbar}\sqrt{\frac{8kT\log 2}{mc^2}}\,,$$

where ΔE_{ij} is the energy of the transition, T the ion temperature and m the mass of the ion. Finally, collisional broadening results in a broadening given by

$$\text{FWHM}_{\text{collisional}} = 2h\nu_{ei}\,,$$

where ν_{ei} is the electron-ion collision frequency. Usually, natural broadening can be neglected, compare with the other two. When both mechanisms, Doppler and collisional, are of importance, the resulting line has a Voigt profile. Its FWHM can be approximated as

$$\text{FWHM}_{\text{voigt}} = 0.5346\text{FWHM}_{\text{collisional}} + \sqrt{0.2166\text{FWHM}^2_{\text{collisional}} + \text{FWHM}^2_{\text{doppler}}}.$$

Figure 2 shows the free electron energy distribution function at the end of the X-ray pulse (200 fs) but before any collisional relaxation process involving them takes place. Three peaks, two corresponding to photoelectrons (1123 eV and 1094 eV) and one to Auger electrons (810 eV) are clearly shown. The temporal evolution of the electron density in the plasma created is also shown. A dense ($n_e > 10^{22}$ cm^{-3}) plasma is created in some tens of femtoseconds.

The adiabatic polarization can be computed from the susceptibility $P = \epsilon_0\chi E$, where $\chi = \chi' - i\chi''$. Its imaginary part is $\chi'' = \dfrac{d^2}{\hbar\gamma\epsilon_0}(N_u - N_l)$ [22]. It is worth mentioning that, when $N_u > N_l$, i.e. a population inversion is created, the susceptibility is positive. Even at these densities and temperatures, Auger ionization dominates the depolarization rate and thus $\gamma = A_{\text{auger}}/2$. The resulting susceptibility is shown in Figure 3. As expected from the population dynamics, the polarization rises in less than 10 fs and then decays steadily, due to the ionization of Ne^{1+} via Auger and photoionization processes, as explained above. Since this decay is due to the ionization of Ne^{1+}, neither the population inversion nor the susceptibility become negative.

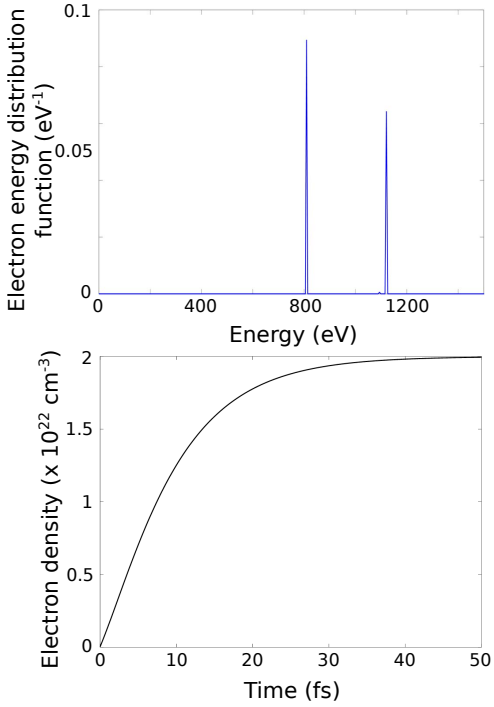

Figure 2. (upper part) Electron energy distribution function. The two photoionization peaks at 1123 eV and 1094 eV (barely visible due to its low intensity) and the Auger peak at 810 eV are visible. (bottom part) Temporal evolution of the electron density of the plasma created.

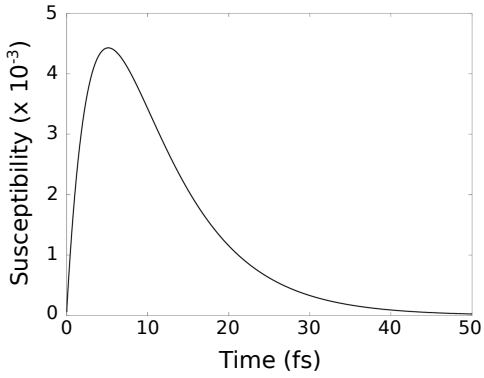

Figure 3. Imaginary part of the adiabatic susceptibility resulting from the population inversion created in Ne^{1+} ions.

As a population inversion and an induced susceptibility have been created, spontaneous emission from the excited level to the ground state of Ne^{1+} ($\hbar\omega = 849$ eV) can propagate and be amplified throughout different clusters. As it was aforementioned, Maxwell-Bloch-Boltzmann formalism is needed to model these processes.

4 Conclusions

In summary, in this paper we present a self-consistent time-dependent Maxwell-Boltzmann-Bloch kintetic model that can be used to model the interaction of intense X-ray pulses from free electron lasers with noble gas clusters and atoms. The strong photoionization induced by the FEL pulse creates a nanoplasma, which is modeled using a Boltzmann equation for the free electrons. The band structure of the clusters taken into account via Boltzmann equations for the carriers while rate equations are used to follow atomic and ionic levels dynamics. Inner core ionization might result in the creation of a population inversion and subsequent amplification of spontaneous emission. This process can be modeled using Maxwell-Bloch equations. Since the transfer of energy from free electrons forming the nanoplasma towards the atomic nucleus is an efficient excitation mechanism, the formalism presented in this paper includes all the required mechanisms to model the plasma formation and the deep level stripping processes as key stages of this phenomenon.

As an example, the irradiation of Ne clusters with an intense X-ray pulse was modeled. The ultrafast photoionization of the ground state of Ne and Ne^{1+} creates a population inversion in Ne^{1+} ions, between its ground state and the $1s^1 2s^2 2p^6$ level. We find that Auger decay towards Ne^{2+} and the aforementioned photoionization of the ground state are responsible of the decay of the population inversion and not the spontaneous emission from the excited state towards the ground state (since it is a slower process). The electron energy distribution function of unbound electrons is also calculated prior to the onset of collisional processes.

Acknowledgments

Support from the Bulgarian National Science Fund under Contract No. DFNI-E02/6 and Contract No. DNTS/FRANCE-01/9 (T.A.) is gratefully acknowledged.

References

[1] S.M. Vinko, et al. (2012) *Nature* **482** 59-62.
[2] G. Gosselin, P. Morel, and P. Mohr (2010) *Phys. Rev. C* **81** 055808.
[3] V. Goldanskii and V.A. Namiot (1976) *Phys. Lett.* **62B** 393.

[4] J. Gunst, Yu.A. Litvinov, C.H. Keitel, and A. Pálffy (2014) *Phys. Rev. Lett.* **112** 082501.

[5] V.P. Krainov and M.B. Smirnov (2002) *Phys. Rep*. **370** 237.

[6] J. Abdallah Jr, J. Colgan, and N. Rohringer (2013) *J. Phys. B: At. Mol. Opt. Phys*. **46** 235004.

[7] D.H. Huang, P.M. Alsing, T. Apostolova, D.A. Cardimona (2005) *Phys. Rev. B* **71** 045204.

[8] J. Abdallah Jr and J. Colgan (2012) *J. Phys. B: At. Mol. Opt. Phys*. **45** 035701.

[9] M. Lindberg and S.W. Koch (1988) *Phys. Rev. B* **38** 3342.

[10] F. Rossi, T. Kuhn (2002) *Rev. Mod. Phys.* **74** 895.

[11] O.Hess, T. Kuhn (1996) *Phys. Rev. A* **54** 3347.

[12] T. Apostolova, J.M. Perlado, A. Rivera (2015) *Nucl. Instr. and Met. B* **352** 167.

[13] S.M. Cavaletto, C. Buth, Z. Harman, E.P. Kanter, S.H. Southworth, L. Young, and C.H. Keitel (2012) *Phys. Rev. A* **86** 033402.

[14] M.F. Gu (2008) *Can. J. Phys.* **86** 675.

[15] P. Ding, J.C. Escudero, A. Houard, A. Sanchis, J. Vera, S. Vicéns, Y. Liu, and E. Oliva (2017) *Phys. Rev. A* **96** 033810.

[16] S.-K. Son, L. Young, and R. Santra (2011) *Phys. Rev. A* **83** 033402.

[17] A.G. de la Varga (2014) Doctoral Thesis, Universidad Politecnica de Madrid.

[18] N. Rohringer, D. Ryan, R.A. London, M. Purvis, F. Albert, J. Dunn, J.D. Bozek, C. Bostedt, A. Graf, R. Hill, S.P. Hau-Riege, J.J. Rocca (2012) Nature **481** 488.

[19] C. Weninger et al. (2013) *Phys. Rev. Lett.* **111** 233902.

[20] J. Abdallah Jr., M.E. Sherrilla, D.P. Kilcreasea, C.J. Fontesb, H.L. Zhangb, J. Oelgoetzb (2009) The reduced detailed configuration accounting (RDCA) model for NLTE plasma spectral calculations,10.1016/j.hedp.2009.05.0061

[21] H.V. Regemorter (1962) *Astrophys. J*. **136** 906.

[22] A. Yariv (1988) "*Quantum Electronics*", 3rd ed. (John Wiley and Sons).